Underestimation of deep convective cloud tops by thermal imagery

Steven C. Sherwood and Jung-Hyo Chae
Department of Geology and Geophysics, Yale University, New Haven, Connecticut, USA

Patrick Minnis
NASA/Langley Research Center, Hampton, Virginia, USA

Matthew McGill
NASA/Goddard Space Flight Center, Greenbelt, Maryland, USA

Received 11 February 2004; revised 9 April 2004; accepted 6 May 2004; published 4 June 2004.

[1] The most common method of ascertaining cloud heights from space is from thermal brightness temperatures. Deep convective clouds of high water content are expected to radiate as black bodies. Here, thermal cloud top estimates from GOES-8 are compared with direct estimates of where the top should be sensed, based on colocated Goddard Cloud Physics Lidar (CPL) observations collected during the Cirrus Regional Study of Tropical Anvils and Florida Area Cirrus Experiment (CRYSTAL-FACE). GOES-8 cloud top heights are consistently ~1 km lower than the "visible" cloud top estimates from the lidar, even though the latter take into account the finite visible opacity of the clouds and any overlying thin cirrus layers, and are often far below the position of highest detected cloud. The low bias in thermal estimates appears to get worse for the tallest clouds, perhaps by an additional kilometer, and depends little on cloud albedo. The consistency of the bias over multiple satellites suggests that cloud retrievals are affected by an unexpected radiative transfer issue. *INDEX TERMS:* 0368 Atmospheric Composition and Structure: Troposphere—constituent transport and chemistry; 3314 Meteorology and Atmospheric Dynamics: Convective processes; 3359 Meteorology and Atmospheric Dynamics: Radiative processes; 3360 Meteorology and Atmospheric Dynamics: Remote sensing. **Citation:** Sherwood, S. C., J.-H. Chae, P. Minnis, and M. McGill (2004), Underestimation of deep convective cloud tops by thermal imagery, *Geophys. Res. Lett.*, *31*, L11102, doi:10.1029/2004GL019699.

1. Introduction

[2] Since the first weather satellites in the 1960's, thermal imagery has been an invaluable source of information on cloud heights and storm severity. One can locate the approximate top of an opaque cloud by observing its effective blackbody temperature ("brightness temperature" T_λ) at some wavelength λ that passes easily through air (e.g., ~10–12 μm), and matching this to a local atmospheric sounding [*Smith and Platt*, 1978] to obtain a height Z_λ. This continues to be a mainstay of cloud-related research, due to the wide availability of infrared data and simplicity of the method. An important complication is that in many cases, emission from below cloud top transmits either through the cloud itself or through gaps, inflating T_λ relative to the true cloud-top temperature. Photon scattering can also affect radiances. Much work has been done on addressing these issues for thin or broken clouds using multiple wavelengths [e.g., *Smith and Platt*, 1978; *Platnick et al.*, 2003; *Minnis et al.*, 1998].

[3] These complications are not thought to be significant for deep convective clouds, due to their high water contents. Errors may arise instead from cloud heterogeneity and cloud-environment temperature differences, but corrections would require detailed information on the cloud, so it is typically just treated as a black body at the environmental temperature. There are indications from case studies [*Heymsfield et al.*, 1991; *Smith*, 1992] that this may underestimate heights by a kilometer or more.

[4] The importance of knowing deep cumulus heights accurately is underscored by some recent developments. For example, intense updrafts are responsible for the creation of hailstones and lighting [*Zipser and Lutz*, 1994]. A wealth of recent data has illustrated how strongly lightning prefers continents, but we still do not know why [*Williams and Stanfill*, 2002]. Cumulus mixing effects near the tropopause, which may be important for tracer transport and energy budgets [*Fromm and Servranckx*, 2003; *Gettelman et al.*, 2002; *Sherwood et al.*, 2003], are also sensitive to small changes in penetration depth. Here we compare thermal cloud top estimates against those expected from cloud opacity information obtained during the Cirrus Regional Study of Tropical Anvils and Florida Area Cirrus Experiment (CRYSTAL-FACE) during July 2002 [*Jensen et al.*, 2004].

2. Computation of Thermal Cb Heights

[5] We obtained 4-km infrared (10.8 μm) brightness temperatures T_{11} taken every 15 minutes by the eighth Geostationary Operational Environmental Satellite (GOES-8). Calibration of the GOES-8 infrared radiances is maintained using on-board blackbodies. The GOES-8 data have also been compared with radiances from similar channels on two research satellites [*Minnis et al.*, 2002] and agree to within ±0.5 K over the full range of temperatures, on average. Cloud temperatures were derived together with other cloud parameters using radiative transfer model parameterizations that account for ice cloud scattering and emission [*Minnis et al.*, 1995,

0094-8276/04/2004GL019699$05.00

1998]. For deep convective clouds of specific interest here, these derived temperatures do not differ significantly from T_{11}.

[6] Cloud heights Z_{11} were determined by two methods. The first, available from the NASA Langley group as a GOES CRYSTAL product (see http://angler.larc.nasa.gov/crystal), uses hourly temperature profiles provided by the Rapid Update Cycle 20-km analyses [*Benjamin et al.*, 2004] by finding the lowest altitude having the estimated GOES-8 cloud temperatures. The second uses several candidate cloud-temperature ($T(Z)$) models based on local radiosonde data to convert T_{11} directly to height. Heights from the two methods do not differ by more than ~100 meters, except for the very tallest clouds where the result begins to depend on the $T(Z)$ model. We present only Z_{11} results from the second procedure. 11 and 12-micron results were similar for optically thick clouds.

[7] Radiosondes were obtained from Key West, Miami, and the CRYSTAL-FACE Western Ground site (81.4W, 25.8N). A "reference sounding" was obtained for each pixel by the following procedure. Pixels near Key West (within about 100 km) were assigned the Key West sounding taken at the nearest available observing time. Those over the peninsula were assigned the mean of the soundings from Miami, the Western Ground site, and Tampa at the nearest available observing time. Other ocean pixels were assigned the mean of all four stations. In general the temperatures did not differ much among the stations, so it's unlikely that significant errors arise from temperature variability on meso- or synoptic scales. Finally, the temperature profiles were smoothed slightly in the vertical using a moving weighted window of width 15 hPa, to reduce features comparable to or smaller than a photon mean free path.

[8] A height Z_{11} was computed for each GOES-8 pixel using the appropriate reference profile, by assigning the lowest altitude where the profile matched the 11 μm brightness temperature T_{11}. This implies an assumption that the cloud temperature will be the same as that of a distant environment at the same altitude. Through most of the troposphere, the interior of thermals tends to be several K warmer than the environment, but this anomaly decreases toward cloud top due to adiabatic cooling and mixing. For overshooting convective clouds, adiabatic cooling dominates and the cloud temperature can be cooler than the environment, by as much as 20 K in the most extreme cases [e.g., *Adler and Mack*, 1986].

[9] We considered this problem by trying three candidate procedures. For "adiabatic-1" we replaced temperatures above the WMO (lapse-rate) tropopause with an adiabat intersecting the observed profile at the tropopause level (the tropopause was typically located near 15 km). "Adiabatic-2" was the same except the adiabat began 40 hPa below the WMO tropopause, far enough down so that the lapse rate was typically near-adiabatic and cloud buoyancies were much more likely to be near neutral. Finally, for the "semiadiabatic" profile we averaged the adiabatic-2 and environmental ones, representing the likely result of a cloud actively mixing with its environment. Over the range of altitudes at which colocated lidar data were available, the choice of profile affected only the very highest cloud top estimates, and these by no more than about 200 meters, so our conclusions are not sensitive to the assumptions.

3. Comparison With Visible Heights

[10] The CRYSTAL-FACE mission included the Cloud Physics Lidar (CPL), which flew on board the NASA ER-2 high-altitude research aircraft. The CPL is a multi-wavelength elastic backscatter lidar that provides cloud and aerosol profiling with 30 m vertical and 1 second temporal resolution. Details of CPL data analysis can be found in *McGill et al.* [2003]. Important features of the CPL design are a small receiver field of view (100 microradians full angle) to minimize multiple scattering, and high sensitivity detectors, revealing thin cloud and aerosol layers that are undetectable by other sensors. Our height estimates differ by less than 50 m in the 532 and 1064 nm channels; we show 1064 nm results since this channel was operational on more flights. The frequent imaging by GOES-8 allows each CPL observation to be co-located to a neighboring satellite pixel taken within eight minutes.

[11] The estimate Z_{11} represents a "radiometric" cloud top. This should occur one photon penetration depth into the cloud if the Planck function $B(\tau)$ is linear in optical depth τ and there is no scattering, as can be seen by substituting such a linear relationship into the solution

$$I_{\mathrm{TOA}} = \int_0^\infty B(\tau) e^{-\tau} d\tau \qquad (1)$$

of Schwarzchild's equation, which yields $I_{\mathrm{TOA}} = B(1)$, or $T_{11} = T(1)$. Numerical evaluation of equation (1) with reasonable nonlinearities in $B(\tau)$ expected for cloud top regions yields T_{11} up to 2 K colder than $T(1)$. Inclusion of scattering may reasonably lead to $T_{11} = T(2) - T(3)$ or so, if scattering goes primarily into a forward peak and the single-scatter albedo is in the range 0.5–0.7. Thus, we should compare Z_{11} with heights determined by the lidar to lie at cloud optical depths of 1–3. This is readily done by integrating the volumetric extinctions provided by the CPL downward from the top of the first aerosol or cloud layer detected, until selected τ values are attained; the resulting heights will be denoted $Z_{\mathrm{lid}}(1)$, $Z_{\mathrm{lid}}(2)$, etc. We refer to $Z_{\mathrm{lid}}(1)$ as the "visible" top.

[12] Figure 1 compares $Z_{\mathrm{lid}}(1)$ with Z_{11} from GOES-8. Each point represents a lidar dwell, colocated to the nearest GOES pixel. Points far off the diagonal are due to optically thin clouds ($Z_{11} < Z_{\mathrm{lid}}(1)$) or points just beyond cloud edges ($Z_{11} > Z_{\mathrm{lid}}(1)$). The central cluster of points comes from thick, beam-filling clouds. In this group a roughly 1-km bias is clearly evident, with Z_{11} too low. The scatter in this group is no greater than 1 km, so this bias is a broad influence on most pixels rather than an episodic error. Comparisons with $Z_{\mathrm{lid}}(2)$ and $Z_{\mathrm{lid}}(3)$ are similar, since these depths typically lie only about 100 and 150 m, respectively, below $Z_{\mathrm{lid}}(1)$.

[13] The lidar loses sensitivity below optical depths of 3–4. Extrapolation based on $Z_{\mathrm{lid}}(2)$ and $Z_{\mathrm{lid}}(3)$ assuming constant opacity would indicate that Z_{11} lies at a visible optical depth of at least 10. The ER-2 also carried two radars, one of which (the 94 GHz Cloud Radar System or CRS) was also sensitive to cloud and had significantly greater penetration than the lidar [see *McGill et al.*, 2004].

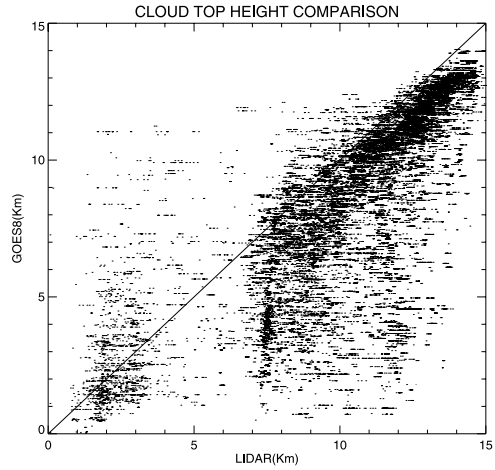

Figure 1. Z_{11} from GOES-8 vs. $Z_{\mathrm{lid}}(1)$ from the CPL lidar. Data come from 20.89 hours of flight time (9.11 hours of good data in cloudy situations) over July 3, 7, 19, 23, and 28.

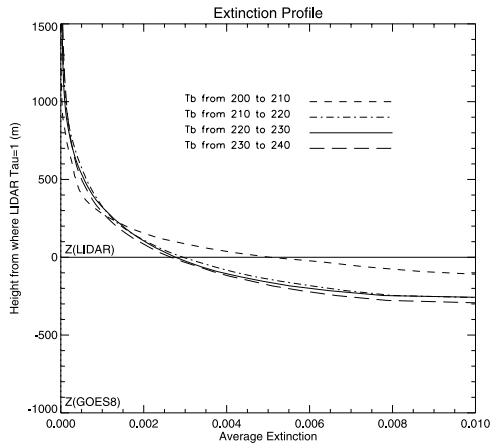

Figure 2. CPL volumetric extinction coefficient averaged as a function of distance above $Z_{\mathrm{lid}}(1)$, for several T_{11} ranges. Typical height of GOES Z_{11} also indicated.

The CRS does not give independent information on optical depth but suggests that cloud opacity typically increases with depth, which would imply that Z_{11} lies at optical depths closer to 20 or 30. It is difficult to explain how an infrared optical depth of unity could coincide with such large visible optical depths.

[14] We must emphasize that the great sensitivity of the lidar does not produce this discrepancy, since we are integrating down through the tenuous upper layers (if present) to get to optically thick levels before comparing with GOES. The height of first cloud detected by the lidar is higher than our "visible top" $Z_{\mathrm{lid}}(1)$ by at least a few hundred meters and often several kilometers. In fact, even the 94 GHz radar consistently detects cloud tops higher than $Z_{\mathrm{lid}}(1)$.

[15] Among the tallest clouds there is an evident tendency for Z_{11} to saturate while $Z_{\mathrm{lid}}(1)$ continues to increase. This tendency was also noted in several supercell thunderstorm overpasses by *Heymsfield et al.* [1991], where overshooting tops (Figures 9–12 from that paper) observed by lidar were not accompanied by commensurate decreases in T_{11} from the earlier GOES-E imager in place at that time. Thus, it would appear that the deepest clouds may be underestimated by closer to 2 km, regardless of the specific GOES imager.

[16] One often assumes that clouds will have a sharp upper boundary, but glaciated clouds typically have fuzzy edges even in regions of active convection. Further, thin laminar clouds may form above the main cumulus cell. Figure 2 shows composite retrievals of volumetric extinction coefficient (a proxy for cloud ice concentration if variations in particle size and shape are neglected) as a function of the distance above $Z_{\mathrm{lid}}(1)$. The lidar shows that cloud material extending above this level decreases in a quasi-exponential manner. Thus, in addition to the 1 km bias, we must reckon on cloud material some distance above the "visible top," even for deep convective clouds.

[17] Efforts to identify cloud properties that are related to the bias met with little success. The cold-cloud bias is about 100 m smaller in Z_{12} than Z_{11}. It persisted stubbornly at all values of cloud albedo (Figure 3), though decreasing slightly for the brightest clouds. The fact that the error does not disappear even for the brightest clouds (whose albedos suggest optical depths $\gg$100) is particularly shocking. The error also shows no correlation with 94 GHz radar cloud top heights, lidar-radar differences, or land vs. ocean.

[18] We have examined "best-winds" stereoscopic visible retrievals of cloud height from the Multiangle Imaging SpectroRadiometer instrument collected in the CRYSTAL-FACE region and time frame (not shown), finding the same 1–2 km discrepancies with thermal imagery. This suggests that MISR "sees" $Z_{\mathrm{lid}}(1)$ and may be of value as an independent source of global deep convective cloud height estimates. Further testing is needed, however, to see how retrievals near the tropopause are affected by the wind shear that is typical there.

4. Discussion

[19] The 5–7 K, 1-km bias between visible and infrared cloud top heights is puzzlingly large, easily standing out above the variability among beam-filling, opaque clouds. It evidently cannot be due to satellite or radiosonde

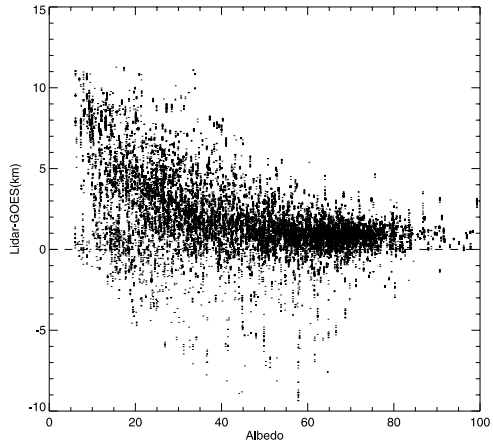

Figure 3. Discrepancy $Z_{\mathrm{lid}}(1) - Z_{11}$ as a function of GOES-derived cloud albedo.

calibration problems, since instrument comparisons limit their uncertainties to an order of magnitude less than needed. We can only list and discuss several other possible sources of error, in no particular order: i) Within-pixel cloud heterogeneity or "beam-filling" errors; ii) finite cloud emissivity; iii) IR scattering and/or differences in visible extinction and IR absorption cross sections; iv) nonlinear emission profile $B(\tau)$; v) cloud-environment temperature differences; vi) stray light in the infrared optics.

[20] Unfortunately, none of these explanations seems satisfactory on its own. Cloud heterogeneity can cause biases due to the nonlinearity of $B(T)$, but tests indicate that heterogeneity on the 1-km scale contributes no more than 1 K of warm bias, and achieving large biases requires that pixels have a mixture of clear sky and thick deep cloud, an occurrence far too rare to explain the results. Models indicate that for cloud temperatures below about 230 K, scattering should not significantly affect T_{11} [*Minnis et al.*, 1998], at least for plane-parallel clouds. The nonlinearity of $B(\tau)$ and cloud-environment temperature differences each produce errors that should make clouds appear too high rather than too low.

[21] Cloud optical depths will be greater in visible than infrared wavelengths if many small particles are present. Particles greater than about 10 μm are in the Mie or geometric-optics scattering regimes for both infrared and visible radiation, which means their extinction cross sections should not (assuming a realistic spread of sizes) differ by more than a factor of two or so between the two wavelengths. Smaller particles begin to enter the Rayleigh regime for infrared radiation, where cross sections rapidly decrease. But to account for Z_{11} at visible optical depths >10, one would need most of the total particle surface area in the upper part of the cloud to be in particle diameters much less than 10 μm, whereas in-situ observations indicate median-area diameters somewhat greater than 10 μm [*Garrett et al.*, 2003]. Instrumental undercounting of small cloud, haze, or aerosol particles would have to be invoked for such an explanation to work.

[22] Stray light or crosstalk from warmer parts of the scene could scatter into the cold pixels, biasing all observations toward the field-of-view mean. Most on-board calibration and many intercomparison procedures would not detect such a problem, but the consistency of the bias across several thermal imagers argues against this explanation in favor of one rooted in cloudy radiative transfer.

[23] In summary, the thermal warm bias remains a mystery. Though small compared to the dynamic range of observed cloud heights, the bias is nonetheless significant from the perspective of differentiating intense storms or quantifying troposphere-stratosphere mixing. We hope that continued research will yield explanations.

[24] **Acknowledgments.** We thank Heidi Zeleznik for data management, Roger Davies for assistance and advice regarding MISR data, Chris Moeller and Tim Garrett for useful discussions, and Dennis Hlavka for assistance with CPL data. This work was supported by NASA EOS/IDS grant NAG-59632 and NAG5-12056.

References

Adler, R. F., and R. A. Mack (1986), Thunderstorm cloud top dynamics as inferred from satellite observations and a cloud top parcel model, *J. Atmos. Sci.*, *43*, 1945–1960.

Benjamin, S. G., D. Dévényi, S. Weygandt, K. J. Brundage, J. M. Brown, G. A. Grell, D. Kim, B. E. Schwartz, T. G. Smirnova, T. L. Smith, and G. S. Manikin (2004), An hourly assimilation/forecast cycle: The Ruc, *Mon. Weather Rev.*, *132*, 495–518.

Fromm, M. D., and R. Servranckx (2003), Transport of forest fire smoke above the tropopause by supercell convection, *Geophys. Res. Lett.*, *30*(10), 1542, doi:10.1029/2002GL016820.

Garrett, T. J., H. Gerber, D. G. Baumgardner, C. H. Twohy, and E. M. Weinstock (2003), Small, highly reflective ice crystals in low-latitude cirrus, *Geophys. Res. Lett.*, *30*(21), 2132, doi:10.1029/2003GL018153.

Gettelman, A., M. L. Salby, and F. Sassi (2002), Distribution and influence of convection in the tropical tropopause region, *J. Geophys. Res.*, *107*(D10), 4080, doi:10.1029/2001JD001048.

Heymsfield, G. M., R. Fulton, and J. D. Spinhirne (1991), Aircraft overflight measurements of midwest severe storms—Implications on geosynchronous satellite interpretations, *Mon. Weather Rev.*, *119*, 436–456.

Jensen, E., D. Starr, and O. B. Toon (2004), Mission investigates tropical cirrus clouds, *EOS*, *85*, 45–50.

McGill, M. J., D. L. Hlavka, W. D. Hart et al. (2003), Airborne lidar measurements of aerosol optical properties during SAFARI-2000, *J. Geophys. Res.*, *108*(D13), 8493, doi:10.1029/2002JD002370.

McGill, M. J., L. Li, W. D. Hart et al. (2004), Combined lidar-radar remote sensing: Initial results from CRYSTAL-FACE, *J. Geophys. Res.*, *109*, D07203, doi:10.1029/2003JD004030.

Minnis, P., D. P. Kratz, J. A. J. Coakley et al. (1995), Clouds and the Earth's Radiant Energy System (CERES) algorithm theoretical basis document, volume III: Cloud analyses and radiance inversions (subsystem 4), in *Cloud Optical Property Retrieval (Subsystem 4.3)*, vol. 3, *Rep. 1376*, edited by the CERES Science Team, pp. 135–176, NASA, Hampton, Virginia.

Minnis, P., D. P. Garber, D. F. Young et al. (1998), Parameterization of reflectance and effective emittance for satellite remote sensing of cloud properties, *J. Atmos. Sci.*, *55*, 3313–3339.

Minnis, P., L. Nguyen, D. R. Doelling et al. (2002), Rapid calibration of operational and research meteorological satellite imagers, part II: Comparison of infrared channels, *J. Atmos. Oceanic Technol.*, *19*, 1250–1266.

Platnick, S., M. D. King, and S. A. Ackerman et al. (2003), The MODIS cloud products: Algorithms and examples from Terra, *IEEE Trans. Geosci. Remote Sens.*, *41*, 459–473.

Sherwood, S. C., T. Horinouchi, and H. A. Zeleznik (2003), Convective impact on temperatures observed near the tropical tropopause, *J. Atmos. Sci.*, *60*, 1847–1856.

Smith, R. B. (1992), Deuterium in North-Atlantic storm tops, *J. Atmos. Sci.*, *22*, 2041–2057.

Smith, W. L., and C. M. R. Platt (1978), Comparison of satellite-deduced cloud heights with indications from radiosonde and ground-based laser measurements, *J. Appl. Meteorol.*, *17*, 1796–1802.

Williams, E., and S. Stanfill (2002), The physical origin of the land-ocean contrast in lightning activity, *C. R. Phys.*, *3*, 1277–1292.

Zipser, E. J., and K. R. Lutz (1994), The vertical profile of radar reflectivity of convective cells—A strong indicator of storm intensity and lightning probability?, *Mon. Weather Rev.*, *122*, 1751–1759.

J.-H. Chae and S. C. Sherwood, Department of Geology and Geophysics, Yale University, New Haven, CT 06520, USA. (ssherwood@alum.mit.edu)

M. McGill, Building 33, Room B424, NASA/Goddard Space Flight Center, Greenbelt, MD 20771, USA.

P. Minnis, Mail Code 420, Building 1250, Room 162, NASA/Langley Research Center, Hampton, VA 23681, USA.